Applied Catalysis A, General 569 (2019) 66–74

Contents lists available at ScienceDirect

Applied Catalysis A, General

journal homepage: www.elsevier.com/locate/apcata

Catalytic self-sustained combustion of toluene and reaction pathway over $Cu_xMn_{1-x}Ce_{0.75}Zr_{0.25}/TiO_2$ catalysts

Chenchen Zhao[a], Qinglan Hao[a], Qing Zhang[a], Ningna Yan[a], Jiaren Liu[a], Baojuan Dou[a,*], Feng Bin[b,*]

[a] Tianjin University of Science & Technology, Tianjin 300457, China
[b] Institute of Mechanics, Chinese Academy of Science, Beijing 100190, China

ARTICLE INFO

Keywords:
Toluene
Self-sustained combustion
Ce-Zr based catalyst
Lean-combustion limit
Reaction pathway

ABSTRACT

The catalytic self-sustained combustion of toluene over $Cu_xMn_{1-x}Ce_{0.75}Zr_{0.25}/TiO_2$ catalysts (x = 1, 0.5, 0) was studied in a microscale combustor. The catalytic activity is determined not only by the temperature with toluene conversion of 90% (T_{co}), but also by the corresponding lean-combustion limits. It was found that the self-sustained combustion was achieved successfully over the catalysts, with the toluene concentrations of 0.35 con.%, 0.50 con.% and 1.00 con.%. According to T_{co}, the activity decreased in the order of $CuCe_{0.75}Zr_{0.25}/TiO_2$ (234 °C) > $Cu_{0.5}Mn_{0.5}Ce_{0.75}Zr_{0.25}/TiO_2$ (238 °C) > $MnCe_{0.75}Zr_{0.25}/TiO_2$ (284 °C). The excellent activity of $CuCe_{0.75}Zr_{0.25}/TiO_2$ catalyst could be ascribed to the high content of active lattice oxygen, good low-temperature reducibility and homogeneous dispersion, combined with the results of H_2-TPR, O_2-TPD and XPS. Furthermore, the results of in-situ DRIFT and temperature-programmed oxidation (TPO) of toluene in N_2 atmosphere suggested that toluene was adsorbed on the catalyst surface by removing α-H from methyl and combining with active oxygen specie to form benzyl group, which was finally oxidized into CO_2 and H_2O with lattice oxygen.

1. Introduction

Toluene is one of the major contributors to VOCs which are mainly released by industries processes. It is hazardous to environment and even carcinogenic for both human and animal [1]. Abundant global technologies based on recovery and destruction have been developed to meet the strict environment regulations of toluene emission limitation.

To accelerate the miniaturization of energy systems and increase the reaction rate, the catalytic combustion in microscale tube, named "catalytic self-sustained combustion", has been developed recently [2]. The technology of stabilizing combustion is an economical strategy for complete VOCs degradation without heat input. In this process, only a small amount of heat is need for the ignition, and the heat released from the reaction is enough to maintain the combustion without any other energy input [3]. Yang [2] and Scarpa [4] found that alkanes including methane, propane and *n*-octane could achieve self-sustained combustion successively over Pt-based catalyst supported ZSM-5 or γ-Al_2O_3 with relatively lower concentration. In addition, the self-sustained combustion can be obtained by CO → CO_2 exothermic reaction over the CuCe/ZSM-5 and $CuCe_{0.75}Zr_{0.25}/TiO_2$ catalysts in our previous studies [5,6].

Catalytic self-sustained combustion of toluene in a small-scale combustor is flameless combustion with a small amount of fuels, which are used to generate the local hot spots on the catalyst surface, leading to the successful self-sustained combustion. The challenge of the technology is to design a proper catalyst to enhance the stability of micro-combustion. Copper-based and manganese-based catalysts are considered as the excellent catalysts for VOCs removal due to their variety of electronic structures and capability of regeneration [7–11]. Copper doping could significantly enhance the catalytic activity to achieve complete VOCs degradation by extracting the lattice oxygen from CuO [8,9]. The MnO_x catalysts for VOCs oxidation have been considered as the better alternative than the expensive noble metal, owing to the coexistence of mixed valance states from −3 to +7 and low toxicity [1,10,11]. Some investigators have tried to prepare bimetallic catalysts to study their high activity through the synergistic effect between the two phases [12–14]. For instance, Li et al. [12] found that $CuMn(y)O_x$/γ-Al_2O_3 exhibited higher catalytic activity (T_{90} = 229 °C) compared with CuO_x/γ-Al_2O_3, MnO_x/γ-Al_2O_3 for toluene oxidation, resulting from the formation of the $Cu_{1.5}Mn_{1.5}O_4$ spinel structure in $CuMn(y)O_x$/γ-Al_2O_3 catalyst. However, the pure Cu-based or Mn-based catalysts are still away from arrival of satisfied catalytic performance to VOCs

* Corresponding authors.
E-mail addresses: bjdou@tust.edu.cn (B. Dou), binfeng@imech.ac.cn (F. Bin).

https://doi.org/10.1016/j.apcata.2018.10.034
Received 27 August 2018; Received in revised form 11 October 2018; Accepted 27 October 2018
Available online 29 October 2018
0926-860X/

combustion due to the poor oxygen storage-release capacity and instability of catalysts. CeO_2 has the unique properties due to the plenty of oxygen vacancies associated with strong interactions with metals, and the adding of CeO_2 can further improve the catalytic performance [5,9,15–17]. The thermal stability of the catalyst can be enhanced through the zirconium addition [15–17]. In our previous study, we have investigated the influence of Cu/Ce molar ratio of CuCe/ZSM-5 catalysts [15] and the Ce/Zr molar ratio of CuCeZr/ZSM-5 catalysts [16] for the catalytic activity, respectively. And we found that the $CuCe_{0.75}Zr_{0.25}O_x$ mixed oxides exhibited excellent catalytic activity in the toluene catalytic oxidation owing to the formation of Cu-Ce-Zr-O solid solution, which improved the redox capability and oxygen storage capacity [15,16], could be favorable for toluene self-sustained combustion.

Many studies have focused on the self-sustained combustion reaction with low-carbon organic compounds, such as CO and C_nH_{2n-2} ($n \leq 4$), however, little statistical evidences related to catalytic self-sustained combustion of aromatic compounds have not been reported yet. In this paper, to acquire the performance of toluene self-sustained combustion over different catalysts, the lean-combustion limit of self-sustained combustion and the efficiency of toluene degradation were studied. $Cu_xMn_{1-x}Ce_{0.75}Zr_{0.25}/TiO_2$ catalysts (x = 1, 0.5, 0) were prepared by the impregnation method, and the physical and structural properties were characterized by H_2-TPR, O_2-TPD and XPS. Furthermore, the in-situ DRIFT experiment was carried out to discuss the possible reaction pathways for toluene catalytic combustion, and the role of lattice oxygen was also proposed based on the results of programmed-temperature oxidation in N_2 atmosphere.

2. Experimental specifications

2.1. Catalyst preparation

A series of $Cu_xMn_{1-x}Ce_{0.75}Zr_{0.25}/TiO_2$ catalysts (x = 1, 0.5, 0) with 4.0 wt.% $Cu_xMn_{1-x}O_y$ supported on TiO_2 (supplied by the Evonik Industries AG), were prepared by the incipient impregnation method. The appropriate amount of $Cu(NO_3)_2{\cdot}xH_2O$, $Mn(NO_3)_2{\cdot}2H_2O$, $Ce(NO_3)_3{\cdot}6H_2O$ and $Zr(NO_3)_4{\cdot}5H_2O$ were well dissolved in deionized water before being added dropwise to nanometer titanium dioxide. The resulting emulsions were dried at room temperature until complete evaporation of the water, then staved at 105 °C for 12 h and calcined in air at 550 °C for 4 h. The molar ratio of Cu_xMn_{1-x}: Ce: Zr was 4: 3: 1, and the Cu_xMn_{1-x}: (Ce + Zr) ratio was 1: 1, which are the optimal ratio from our previous works [15,16].

Finally, all the catalysts were sieved in a size of 20–30 meshes for testing. The obtained catalysts were named as $CuCe_{0.75}Zr_{0.25}/TiO_2$ (CuCZ/T), $Cu_{0.5}Mn_{0.5}Ce_{0.75}Zr_{0.25}/TiO_2$ (CuMnCZ/T) and $MnCe_{0.75}Zr_{0.25}/TiO_2$ (MnCZ/T).

2.2. Catalyst characterization

The Powder X-ray diffraction (XRD) data was performed on XRD-6100 (Shimadzu, Japan) equipped with X-ray diffractometer using Cu-Kα (λ = 1.540 Å, 40 kV). The measurements were conducted in the 2Θ range from 5° to 80° with a scanning rate of 2°/min. Hydrogen temperature programmed reduction (H_2-TPR) was measured with a PCA-140 instrument (Bolider). To eliminate contaminants, 200 mg sample was pretreated at 500 °C for 1 h in argon (50 mL/min). After the temperature was cooled to 50 °C, the TPR analysis were performed in 5 vol. % H_2/Ar (50 mL/min) at the temperature programmed (10 °C/min) in the range of 50–800 °C. The reduction degree (R_d) of the catalysts was calculated by the ratio of the hydrogen consumption of $CuMnO_x$ and theoretical content (4%) in the catalysts. Temperature-programmed desorption of O_2 (O_2-TPD) data was also collected with the same instrument. To remove moisture, a cold trap was introduced before the released gas entered the thermal conductivity detector (TCD). The same amount of catalyst was placed in a pure oxygen flow (50 mL/min) for 1 h at 500 °C. Subsequently, the catalyst was heated from room temperature to 1000 °C at a rate of 10 °C/min under the Ar atmosphere. TCD was employed to continuously monitor the consumption of oxygen. X-ray photoelectron spectra (XPS) was measured with a Perkin-Elmer PHI-1600 ESCA spectrometer. The X-ray source was an Mg anode target (350 eV). The binding energy values of each species were corrected with an internal standard of C1 s (Eb = 284.8 eV).

2.3. In-situ DRIFT

The in-situ diffuse reflectance Fourier transform (DRIFT) result of the toluene combustion over CuCZ/T catalyst was analyzed by using a Bruker Tensor 27 spectrometer equipped with MCT detector. Prior to all measurements, the CuCZ/T catalyst was pretreated in the high-purity N_2 atmosphere (50 mL/min) at 300 °C for 0.5 h. The toluene gas was bubbled into the reactor by oxygen flow (30 mL/min), and the corresponding sample spectrum was recorded until the catalyst was saturated by the toluene adsorption. DRIFTS were probed with the temperature interval of 10 °C from 50 °C to 400 °C under O_2 and toluene gas.

2.4. Catalytic activity measurement

Toluene catalytic self-sustained combustion experiment was carried out in a micro-reactor made of quartz tube (Ø = 6.0 mm × 1.0 mm, L = 200 mm). The experimental set-up of toluene catalytic self-sustained combustion includes continuous flow gas supplying systems, catalytic self-sustained combustion reactor and gaseous analytical systems (Fig. 1). The flow rates of toluene and air were controlled by mass flow controllers, which are shown as MFC1 (F1) and MFC2 (F2) in Fig. 1, respectively, with a full-scale measurement accuracy of ± 1%. The toluene concentration was controlled by adjusting the flow rate of F1 (10 ~ 50 mL/min) and F2 (150 ~ 190 mL/min) while keeping the total flow rate constant (200 mL/min).

The reactor filled with 200 mg catalyst was first heated for ignition, then the heat supply was turned off to observe the combustion running auto-thermally. During the reaction process, the temperature of reactor wall was measured by using an infrared thermography (T640, FLIR, USA). The judgment of catalytic self-sustained combustion in the experiment is based on the variation of the wall temperature, which is

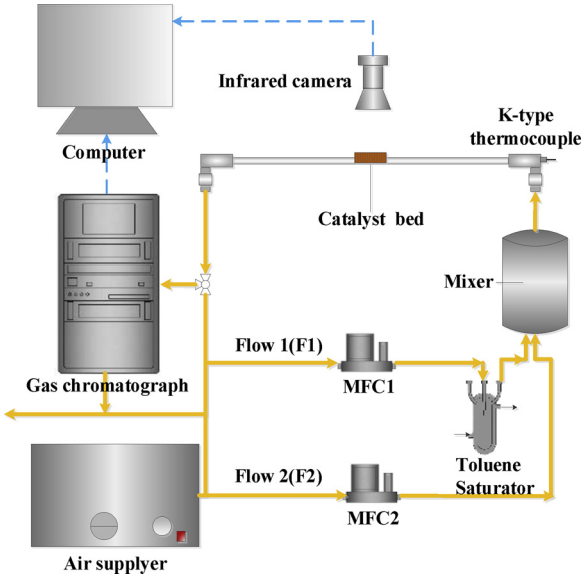

Fig. 1. Schematic of the experimental set-up for toluene self-sustained combustion.

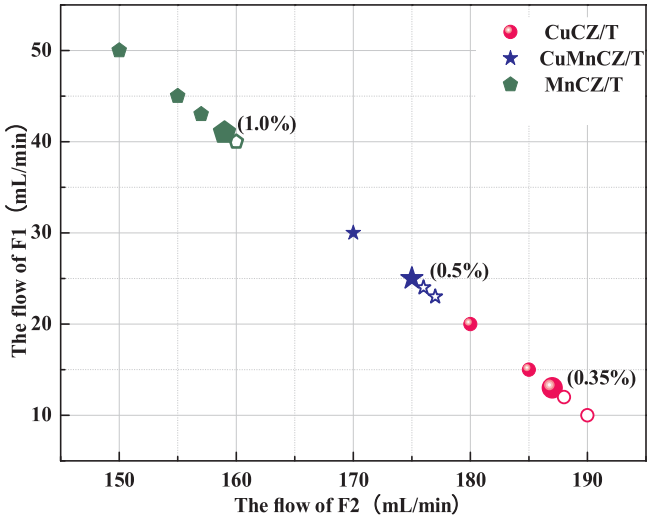

Fig. 2. Lean-combustion limits of toluene self-sustained combustion over CuCZ/T, CuMnCZ/T and MnCZ/T catalystsc.

higher than the room temperature with a range of ± 2 °C in 10 min. The activity of the catalyst can be estimated in terms of the lean-combustion limit (the lowest concentration required for toluene self-sustained combustion over the catalyst) in the combustion. Meanwhile, it can also be measured by the toluene conversion.

3. Results and discussion

3.1. Lean-combustion limits and catalytic activities of toluene self-sustained combustion

The lean-combustion limits with different catalysts for toluene self-sustained combustion in the micro-reactor were investigated by progressively decreasing the toluene concentration (described in Section 2.4) until the process was quenched, and the results are shown in Fig. 2. It can be seen from the figure that the lean-combustion limits over CuCZ/T, CuMnCZ/T and MnCZ/T are 0.35%, 0.50%, and 1.00%, respectively. The lean-combustion limit is in direct proportional to the catalyst activity [4,5].

Table 1
The ignition, light-off and complete combustion of toluene catalytic combustion.

Catalyst	C_7H_8 concentration (%)								
	0.35			0.50			1.00		
	T_{ig}	T_{lo}	T_{co}	T_{ig}	T_{lo}	T_{co}	T_{ig}	T_{lo}	T_{co}
CuCZT	187	224	234	180	226	234	190	228	236
CuMnCZ/T	196	228	238	184	230	238	216	233	243
MnCZ/T	230	273	284	229	276	288	237	285	296

T_{ig}: the ignition temperature required for 10% conversion of toluene at the heating process.
T_{lo}: the light-off temperature which 50% toluene conversion is achieved at the heating process.
T_{co}: the complete temperature that the conversion of toluene is 90% at the heating process.

Fig. 3 illustrates the toluene conversion in the fixed bed with the different lean-combustion limit, and the corresponding T_{ig}, T_{lo} and T_{co} are listed in Table 1. In Fig. 3(A), for instance, when the toluene concentration at 0.35 con. %, T_{co} of CuCZ/T, CuMnCZ/T and MnCZ/T catalysts are 234 °C, 238 °C and 284 °C, respectively. In addition, the heat lines of toluene conversion shift toward higher temperature with the increase of toluene concentration and manganese content in catalysts. It is worth noting that the toluene conversion over CuCZ/T remains at 100% even if the temperature drops below 50 °C during the cooling process, which is evident that the heat released from reaction can maintain the stable combustion. Comparing the results of lean-combustion limit with the T_{co} of different catalysts, it is implied that the catalytic activity of CuCZ/T is the best, with the decrease order of CuCZ/T > CuMnCZ/T > MnCZ/T. The phenomenon observed is different with Xin et al [9] in *Introduction*, and the synergistic effect between Cu and Mn species was failed to show in CuMnCZ/T catalyst used in this work. A possible reason for better activity of CuCZ/T is due to the strong interaction between copper oxide and titanium dioxide. Highly dispersed copper oxide is converted to low-valent copper ions by $Cu^{2+} + Ti^{3+} \rightarrow Cu^{+} + Ti^{4+}$. The existence of Cu^{+} could be more beneficial for surface adsorbed oxide ion to trap electrons through the following process: $Cu^{+} + O_{ads} \rightarrow O_{ads}^{-} + Cu^{2+}$, which promotes the

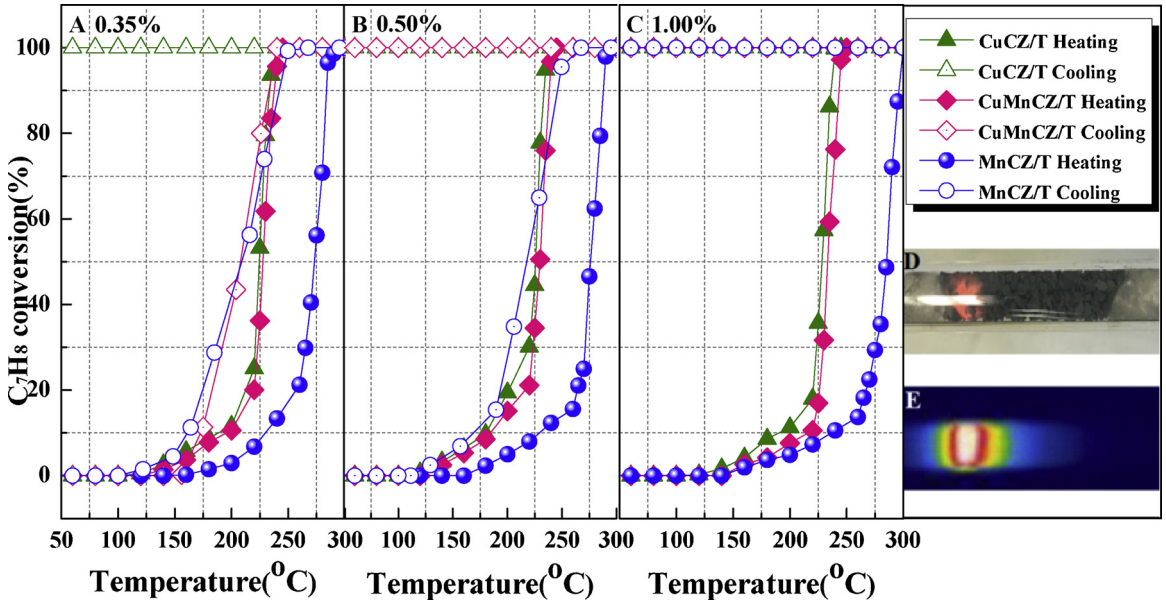

Fig. 3. Activity of toluene catalytic combustion with different lean-combustion limit of 0.35 con. % (A), 0.50 con. % (B), 1.00 con. % (C) and the recorded combustion image (D) and the corresponding temperature distribution (E).

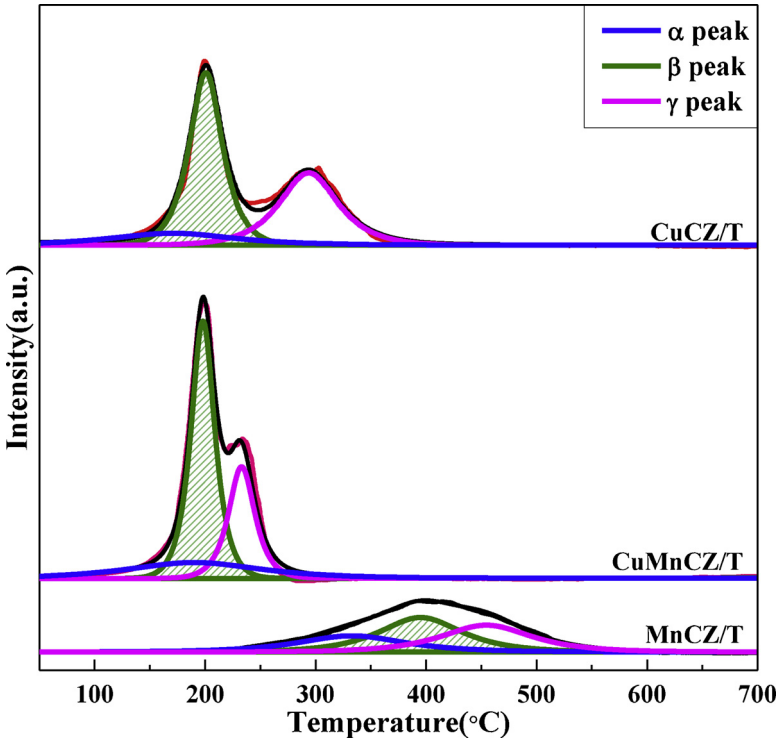

Fig. 4. H_2-TPR patterns of CuCZ/T, CuMnCZ/T and MnCZ/T catalysts.

Table 2
The relative intensity of the reduction peaks on the H_2-TPR curves.

Catalysts	H_2 consumptions (μmol·g^{-1})				
	α peak	β peak	γ peak	Total	R_d (%)
CuCZ/T	25.7 ± 0.4	98.2 ± 0.8	70.6 ± 0.5	194.5 ± 1.7	38.9
CuMnCZ/T	36.5 ± 0.5	104.5 ± 0.9	50.3 ± 0.6	191.3 ± 2.0	53.1
MnCZ/T	29.3 ± 0.4	45.9 ± 0.6	41.5 ± 0.6	116.7 ± 1.6	41.4

∗The degree of the uncertainty was calculated by equations (1) in the supporting information.

formation of radicals with strong oxidizing properties, resulting in an improvement of the activity of the catalyst [18]. Another reason might be that there was low content of $CuMnO_x$ (4%) in the process of catalyst preparation, and CuO_x species are prior to form the Cu-Ce-Zr-O solid solution with Ce and Zr species detected by H_2-TPR, thus limiting the Mn species interacting with CuO_x to form the Cu-Mn spinel.

In the toluene self-sustained catalytic combustion, the continuous combustion can be achieved by the heat released from the reaction, and no external heating is required. The catalyst with lower activity needs higher toluene concentration for affording higher ignition temperature and achieving intense exothermic reaction rapidly. Take CuCZ/T for instance (Fig. 3A), the heating process of catalytic self-sustained combustion can be divided into three steps. The first step is described as an induction process with which the toluene conversion increases slowly at a lower temperature ($< T_{ig}$ = 187 °C). Here, the consumed reactants can be quickly supplemented by the internal diffusion, as embodied in the temperature of the catalyst bed near the setting temperature. When the sufficient power is generated from reaction exothermicity in comparison to the heat dissipation in the process, the toluene conversion is fast enough to ignite, occurring at local hot points of catalyst surface. The accumulation of heat induces a steep increase of the local temperature and reactant rates, then the flame spreads rapidly in the catalyst bed to enter the second step - - transient light-off period ($< T_{ig}$–T_{lo} (224 °C)). Here toluene oxidation rate is increasing to lead a thermochemical runaway reaction, which consequently expedites the external diffusion and mass transfer. In the third step (self-sustained combustion stage), the combustion reaction rate is mainly controlled by the toluene and O_2 diffusion rather than temperature on the catalyst surface [19]. In cooling process, the heat transfer between the surrounding and the wall of the combustion reactor is based mainly on radiation heat transfer, and the nature convection is minor. The lower lean-combustion limit of toluene over CuCZ/T catalyst, which generates less heat in exothermic reaction, is favorable to minimize the temperature gradient between the reactor wall and the surroundings. Consequently, it can allow the stability of micro-combustion based on the heat accumulated by the reaction.

3.2. Catalyst characterization

3.2.1. XRD analysis of catalysts

The XRD patterns of CuCZ/T, CMCZ/T and MnCZ/T catalysts were shown in Fig. S1 (supporting information). All the reflections exhibited in the samples are in agreement with the typical diffraction patterns of TiO_2 (P25). No additional peaks were observed in the patterns indicating that the presence of highly dispersed species of metal oxides supported on TiO_2 or the possible formation of amorphous or nanocrystalline of metals which are too small to be detected by XRD. Therefore it could not be deduced with the cell parameters. There, the content of $Cu_xMn_{1-x}O_{2-\delta}$, CeO_2 and ZrO_2, which were calculated before the preparation of the catalysts, are 4.0%, 8.1% and 5.8%, respectively.

3.2.2. H_2-TPR analysis of catalysts

The redox properties of CuCZ/T, CuMnCZ/T and MnCZ/T catalysts investigated by H_2-TPR are displayed in Fig. 4 (The TPR patterns of pure CuO, MnO_2 and $CeZrO_x$ are presented in Fig. S2). In Fig. S2, the reduction of pure CuO is observed at 150–350 °C and characterized by two overlapping peaks at 240 and 264 °C. The peak at lower temperature is attributed to the reduction of highly dispersed CuO_x on the surface of catalyst, including the isolated Cu^{2+} and the small-scale copper clusters with two dimensions and three dimensions structures. And another peak represents the reduction of Cu^+ species [20]. For

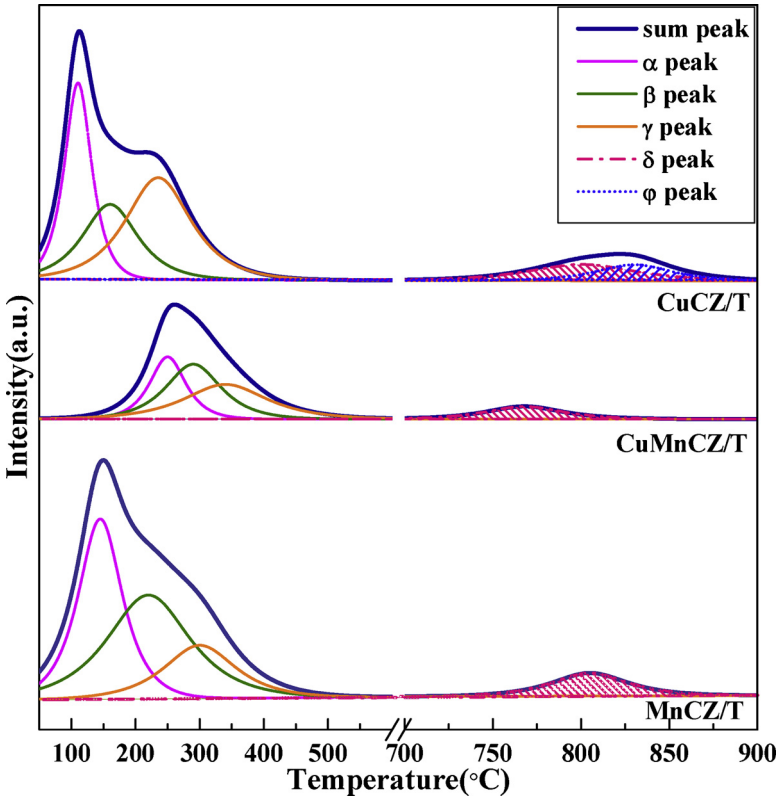

Fig. 5. O_2-TPD patterns of CuCZ/T, CuMnCZ/T and MnCZ/T catalysts.

Table 3
The relative intensity of the desorption peaks on the O_2-TPD curves.

catalysts	O_2 consumption (μmol·g^{-1})				
	adsorbed oxygen			surface lattice	
	α peak	β peak	γ peak	δ peak	φ peak
CuCZ/T	8.0 ± 0.3	6.0 ± 0.2	10 ± 0.4	1.0 ± 0.4	0.7 ± 0.4
CuMnCZ/T	4.0 ± 0.1	5.0 ± 0.2	1.0 ± 0.2	0.5 ± 0.2	–
MnCZ/T	12 ± 0.4	13 ± 0.4	6.0 ± 0.2	1.0 ± 0.2	–

pure MnO_2, there is only a broad hydrogen consumption below 500 °C related to the reduction of MnO_2. The hydrogen consumption of $CeZrO_x$ are shown a single reduction peak at 400–700 °C attributed to the partial reduction of Ce^{4+} to Ce^{3+} at the surface and bulk of the Ce-Zr-O solid solution [21], is not detected in the TPR profiles of catalysts (Fig. 4).

As shown in Fig. 4, the reduction peaks for all the catalysts can be divided into three peaks, labeled as α, β and γ. The reduction of CuO in CuCZ/T catalyst takes place at the lower temperature than the pure CuO species, including the main peak (β) at the range of 150–270 °C and a smaller peak (γ) at 200–400 °C. The addition peak (α) at the lowest temperature about 170 °C can be ascribed to the reduction of the CuO_x species that interact with ceria [13]. The dispersed CuO_x species could incorporate into the cubic vacant sites of ceria and form a five-coordinated surface structure with the capping oxygen, and this unsteady structure can promote the reduction of the CuO_x species and the surface oxygen [22]. For CuMnCZ/T catalyst, the attributions of three peaks are similar to that of CuCZ/T, including the α peak (50–350 °C), β peak (150–250 °C) and γ peak (200–300 °C). According to the literature, it is attributes to the reduction of the CuO_x and MnO_x [20]. But it is difficult to distinguish the peak corresponding to copper or manganese species because the peaks were overlapping with each other. However, MnCZ/T is reduced difficultly in comparation with other catalysts because of its low free energy to form the MnO_x [13]. The three peaks observed for MnCZ/T at 300–500 °C is similar to the pure MnO_2. It is divided into the three peaks, labeled α (200–400 °C), β (250–500 °C) and γ (300–550 °C), are related to the reductions of MnO_2, Mn_2O_3 and the Mn_3O_4, respectively [12].

The corresponding H_2 consumptions and the R_d of $CuMnO_x$ are listed in Table 2. It is suggested that the reduction of $Mn^{4+} \rightarrow Mn^{3+}$ might occur at the lower temperature to increase the H_2 consumption of β peak in CuMnCZ/T catalyst [22]. Addition of Mn to CuCZ/T slightly modified the redox ability of catalyst and promoted the reduction at lower temperature. That can be explained by the fact that an amount of MnO_x doped with CuO can form the lattice defects and oxygen vacancies, and consequently enhance the transfer of oxygen species to promote each other's reduction ability [23]. The total hydrogen consumption of the CuMnCZ/T(191.3 ± 2.0 μmol·g^{-1}) is similar to that on the CuCZ/T(194.5 ± 1.7 μmol·g^{-1}), which are higher than that of MnCZ/T (116.7 ± 1.6 μmol·g^{-1}). The reason probably is due to that the more content of easier reduction Mn^{4+} ions of CuMnCZ/T catalyst in comparison with MnCZ/T [24], which were detected by XPS. It is also consistent with the performance of catalytic activity to some extent.

From the Table 2, the results showed that the R_d of catalysts with the decrease order of CuMnCZ/T (53.1%) > MnCZ/T (41.4%) > CuCZ/T (38.9%). In this work, the T_{ig} and T_{co} of toluene self-sustained combustion are below 300 °C. However, manganese starts to be reduced when the temperature is higher than 300 °C. Probably it is the main reason that catalysts with manganese has the higher reduction degree and the lower activity. Hence, the catalytic activity is mainly related to the reduction temperature of catalysts, and is little affected by the reduction degree.

3.2.3. O_2-TPD spectra of the catalysts

The O_2-TPD profiles of the CuCZ/T, CuMnCZ/T and MnCZ/T samples are shown in Fig. 5, and the relative intensity of the desorption

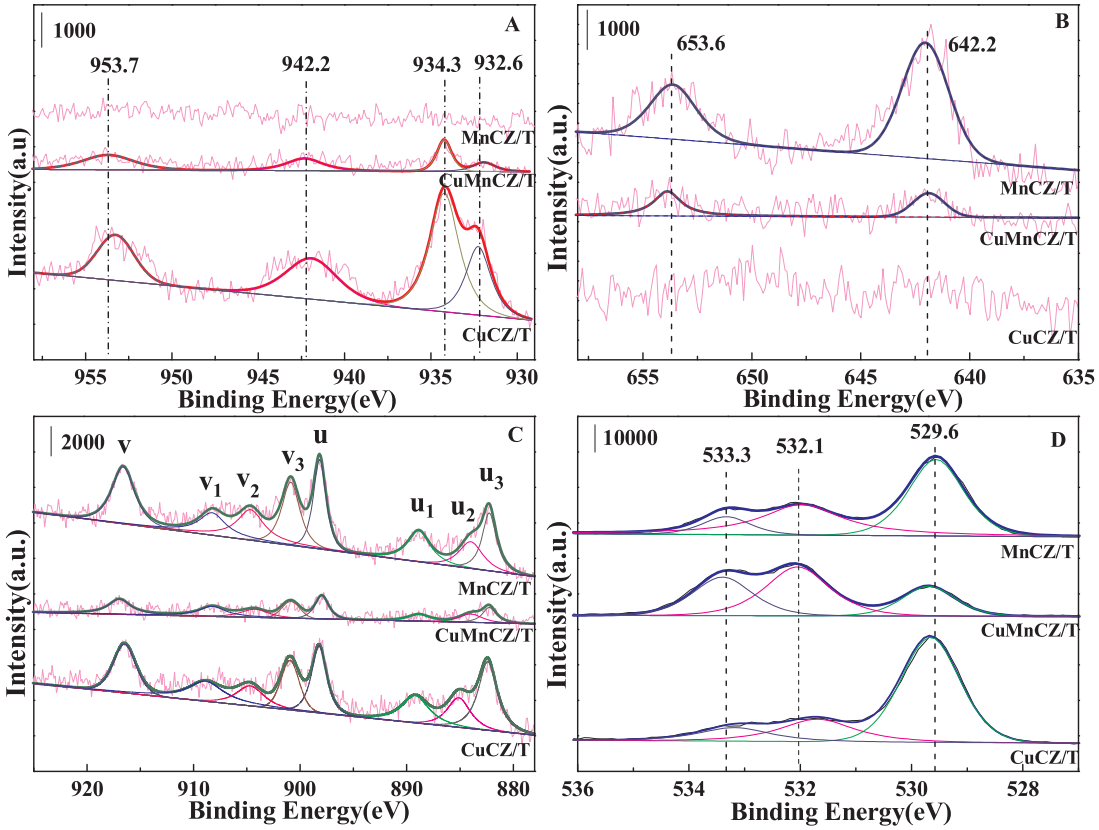

Fig. 6. XPS patterns of Cu 2p (A), Mn 2p (B), Ce 3d (C), and O 1 s (D) for CuCZ/T, CuMnCZ/T and MnCZ/T catalysts.

Table 4
The surface species of CuCZ/T, CuMnCZ/T and MnCZ/T catalysts.

Caralyst	(Cu + Mn)/Ti%	Cu^{+} /Cu^{2+}	Ce^{3+}/Ce^{4+}	Oxygen Species (%)		
				O_{ad}	O_{la}	O_{la}/O_{to}
CuCZ/T	2.00 ± 0.06	0.31 ± 0.02	0.35 ± 0.02	11 ± 1	76 ± 2	87.36 ± 0.10
CuMnCZ/T	2.58 ± 0.07	0.26 ± 0.01	0.31 ± 0.02	32 ± 1	67 ± 1	67.67 ± 0.33
MnCZ/T	1.60 ± 0.09	–	0.25 ± 0.01	14 ± 1	85 ± 2	85.54 ± 0.27

Ola = Ola,r + Ola,c, Oto = Oad + Ola = 99%.

peaks on the O_2-TPD curves are listed in Table 3. The catalysts exhibit similar spectra and can be distinguishably classified into two types of oxygen species, namely, the adsorbed oxygen located at surface vacancies below 550 ℃ and the surface lattice oxygen at the higher temperature between 700 ℃ and 900 ℃. The first broad peak can be divided into three characteristic peaks (denoted as α, β and γ peak) differentiated by the strength of the catalyst surface, which are attributed to the weakly adsorbed oxygen species, O_2^- and O^- species formed by the adsorbed O_2 [25]. The δ and φ peaks are assigned to lattice oxygen species (O^{2-}) [26]. The lattice oxygen is considered as a major participator in deep oxidation of toluene, which is deeply discussed in Section 3.3. Compared with CuMnCZ/T (0.5 μmol g^{-1}) and MnCZ/T (1.0 μmol g^{-1}), CuCZ/T has the highest content of lattice oxygen (1.7 μmol g^{-1}), indicating a largest amount of active oxygen centers for the catalyst. The higher concentration of Ce^{3+} of CuCZ/T catalyst, which was detected by XPS, can promote the migration of the lattice oxygen from the bulk to the surface of catalyst. Sequentially, more active oxygen centers to facilitate the mobility of the lattice oxygen [25]. Obviously, the desorption peak of δ for CuMnCZ/T shifts slightly to lower region in comparison with CuCZ/T and MnCZ/T. The phenomenon can be explained by the fact that the presence of the appropriate amount of Mn enhances the formation of Cu-Mn-Ce-O ternary oxide solid solution with fluorite structure, thereby strengthens the capacity of the active center of oxygen [21].

3.2.4. XPS measurements

XPS is used to characterize the Cu, Mn, Ce and O oxidation state for CuCZ/T, CuMnCZ/T and MnCZ/T catalysts, and the results are depicted in Fig.6. The Cu 2p spectrum for the catalysts represents two main peaks of Cu $2p_{3/2}$ (933.6 eV) and Cu $2p_{1/2}$ (953.7 eV) in Fig. 6A. After the peak deconvolution, the coexistence of Cu^{+}/Cu_2O and Cu^{2+}/CuO are well evidenced by the main peaks at 932.6 eV with a shoulder peak observed at 934.3 eV. The shake-up satellites of Cu at about 942.2 eV are assigned to the divalent copper [27]. The Mn 2p spectra exhibits two contributions of Mn $2p_{3/2}$ and $Mn2p_{1/2}$ located at 642.2 eV and 653.6 eV in Fig. 5B, corresponding to Mn^{3+} and Mn^{4+} ions, respectively [12].

In Fig. 6C, the Ce 3d spectra is distinguished into Ce $3d_{5/2}$ and Ce $3d_{3/2}$ (labeled as u and v, respectively) performing the Ce^{3+}/Ce^{4+} electron-pair. The four intense peaks at u (898.1 eV), v (916.6 eV), u_3 (882.3 eV) and v_3 (900.9 eV) with the two weak peaks at u_1 (888.9 eV) and v_1 (908.3 eV), can be attributed to the different Ce 4f electron configurations in the final states of the Ce^{4+} species. The u_2 and v_2 peaks presented at 904.7 eV and 884.1 eV belong to the Ce^{3+} species

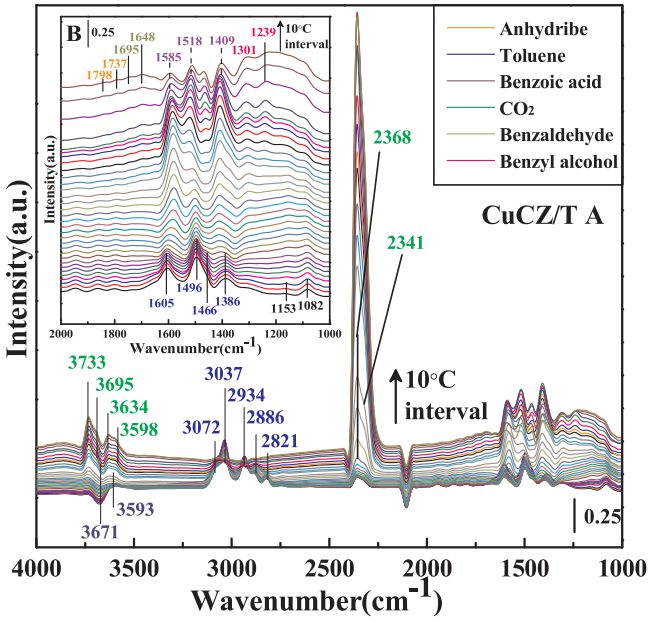

Fig. 7. The in-situ DRIFT spectra of toluene oxidation over CuCZ/T catalyst. (A) The wavenumber range of 1000 ~ 4000 cm^{-1}. (B) The wavenumber range of 1000 ~ 2000 cm^{-1}.

[16], which is due to the entrance of copper/manganese ions into the CeO_2 lattice causing lattice imperfection and generating trivalent cerium ions [27].

The O 1 s spectra of the three catalysts is clearly resolved into three peaks by deconvolution (Fig. 6D), proving the presence of three chemical environments for oxygen atoms. The value of 529.6 eV is generally accepted as being a feature of the characteristic lattice oxygen ($O_{la,m}$) bonded to copper, manganese, cerium and zirconium cations. The second one at higher binding energies (532.1 eV), with lower intensity, is the characteristic of the regular lattice oxygen ($O_{la,t}$) of TiO_2, and the shoulder peak at 533.3 eV indicates the presence of chemisorbed oxygen (O_{ad}) [27].

The related description for the XPS data is listed in Table 4, including the surface species of (Cu + Mn)/Ti, Cu^+/Cu^{2+}, Ce^{3+}/Ce^{4+} and atomic ratio of the CuCZ/T, CuMnCZ/T and MnCZ/T catalysts. It is observed that the contents of (Cu + Mn)/Ti for the obtained catalysts are less than the theoretical value (loading 4.0 wt%), which confirms that the Cu and/or Mn ions are introduced into CeO_2-ZrO_2 lattice and the lattice imperfections are formed. The higher Cu^+/Cu^{2+} ratio in CuCZ/T (0.31) compared to CuMnCZ/T (0.26) provides the evidence of the interaction between divalent copper ions and titanium ions. Consequently, the cerium species with lower oxidation states via the redox equilibrium of $Cu^+ + Ce^{4+} \leftrightarrow Cu^{2+} + Ce^{3+}$ [5,28], improve the ratio of Ce^{3+}/Ce^{4+} (0.35) in CuCZ/T, which is higher than that in CuMnCZ/T (0.31). The presence of more Cu^+ species in the catalysts can promote the catalytic performance for the oxidation reaction. The replacement of Ce^{4+} from Ce^{3+} can form the defect structure, resulting in the oxygen vacancies and unsaturated chemical bonds on the catalyst surface, and bringing the transfer of more chemisorbed oxygen species in ceria into lattice oxides for charge balance [28]. O_{la} species is the main participator in the process of toluene oxidation according to MVK reaction mechanism. Consequently, the highest O_{la} ratio is up to 87.36% in CuCZ/T compared with 67.67% in CuMnCZ/T catalyst, indicating the lattice oxygen species relative concentration increases with the content of copper. The result is confirmed by O_2-TPD.

3.3. Reaction pathway of toluene catalytic combustion

The catalytic combustion of toluene can generate some intermediate products before complete oxidation into CO_2 and H_2O. In our previous work, the analysis of intermediate species combined with the Mars–van Krevelen (MVK) mechanism could explain the oxidation performances of ethyl acetate and toluene on CuCZ/T catalyst to some extent [17]. However, the specific reaction pathways including the adsorption and oxidation of toluene are still not clear.

In this study, the in-situ DRIFT was used to further analyse the reaction process of toluene catalytic combustion over the CuCZ/T catalyst, and the results are shown in Fig. 7. The samples were saturated under the toluene-oxygen atmosphere at the room temperature, until the changeless intensity of the characteristic IR bands associated with toluene, including the bands at 3100–2800 cm^{-1} (the stretching vibration of C—H groups), and the bands at 1610–1380 cm^{-1} (the typical aromatic ring vibration) [29]. It is worth noting that the bands at 2934 and 2886 cm^{-1} are assigned to the methylene rather than methyl, because the symmetric and asymmetric C—H stretching vibration of the CH_3 group is usually observed in the 2970–2950 cm^{-1} region [10]. The appearance of weak bands at 1153 and 1082 cm^{-1} are probably

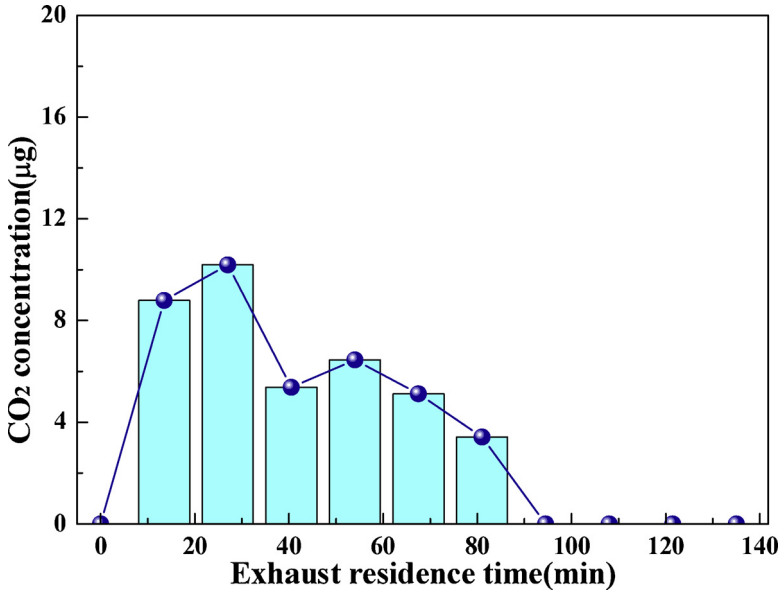

Fig. 8. The toluene combuston over CuCZ/T catalyst in N_2 (160 ℃).

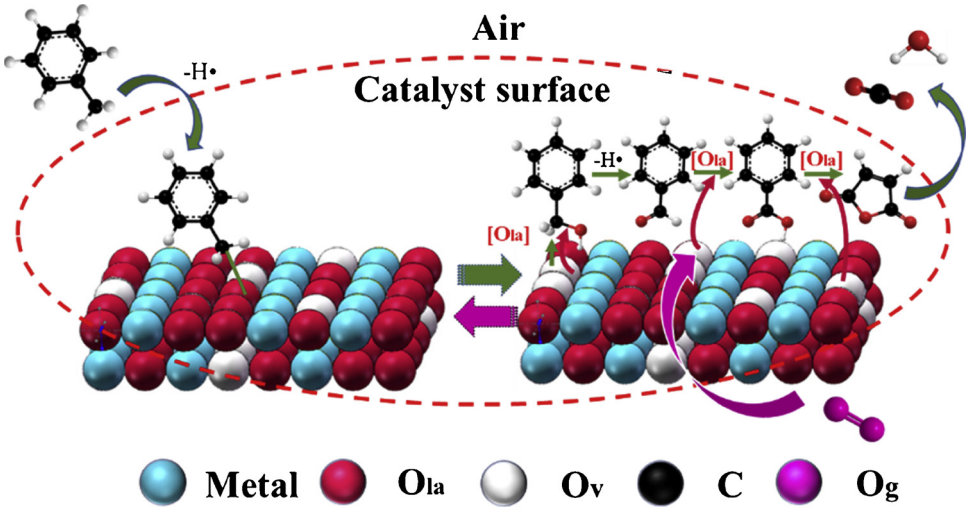

Fig. 9. The reaction pathway of toluene combustion.

ascribed to a C—O vibration mode [10]. These results suggest that toluene is adsorbed on the CuCZ/T surface via the cleavage of the α-H bond in the methyl group of toluene to form the benzyl species, which are subsequently combined with the active oxygen on the catalyst surface through the formation of benzoyl oxide species (C_6H_5-CH_2-O) [10,30]. In addition, the positions of these bands do not shift to lower frequency compared with the spectra of liquid- or gaseous toluene. This phenomenon also testifies that the toluene is adsorbed on CuCZ/T surface via the $-CH_3$ rather than the aromatic ring, because the interaction between the aromatic ring of toluene and the surface of TiO_2 can lead to an obvious blue shift by forming π-complex [10]. The negative band at 3671 cm^{-1} and the band at 3593 cm^{-1} are caused by the surface hydroxyl group interacting with the methyl group of toluene [31], and it confirmsthe methyl group of toluene is adsorbed on catalyst once again.

Under low temperature conditions, hydroxyl groups adsorbed on the catalyst surface occupy the active sites, which hinders the futher oxidation of toluene. In Fig. 7A, it can be seen that when the band at 3593 cm^{-1} disappears, the signals of CO_2 (2368 and 2341 cm^{-1}) [5] increase rapidly with the decreasing of the toluene signals. In addition, the new bands appearing at 1301 and 1239 cm^{-1} (Fig. 6B) are attributed to the methylene group and the C—O vibration mode of benzyl alcohol [29]. With the temperature increasing, the occurrence of the strong peaks at 1585, 1518 and 1409 cm^{-1} resulting from the carboxylate group suggests the production of benzoic acid [32]. Furthermore, the weak bands at 1695 and 1648 cm^{-1} designated to aldehydic species are also tracked. And the weak bands at 1798 and 1737 cm^{-1} imply the appearance of anhydride species [25]. The band intensities of benzoic acid, aldehydic and anhydride species continuously increase with the increasing of temperature. Noticeably, with the reaction temperature higher than 350 ℃, the intensities of CO_2 bands are significantly higher than the others. According to the integral of the band areas at 400 ℃, the formation of CO_2 has a approximately ratio of 98%, which demonstrates that CO_2 is the dominant product of toluene catalytic oxidation with traces of benzoic acid, aldehydic and anhydride species as by-products.

To investigate whether the lattice oxygen participates in the combustion of toluene or not, the experiment of the toluene combustion over CuCZ/T catalyst (0.8 g) at 160 ℃ (the temperature at which CO_2 can be tracked firstly through GC) in N_2 atmosphere was carried out, and the results are depicted in Fig. 8. The sample was first pretreated with N_2 for 0.5 h at 400 ℃ to eliminate the effects of surface oxygen species. Although the reactants contain no gas-phase oxygen, CO_2 was still detected by GC, which proves that lattice oxygen is in the involvement of the deep catalytic oxidation of toluene, in accordance with the previous result found by Sun et al. [10]. Furthermore, the amount of lattice oxygen consumed in the reaction by integral shows a good qualitative agreement with the peak area of lattice oxygen investigated by O_2-TPD.

To sum up, combining with our previous study [17], the model established on the MVK reaction mechanism provides a good fit for the toluene combustion over CuCZ/T. Based on the redox process, there are two steps in the MVK model. Firstly, adsorbed toluene reacts with the lattice oxygen on the catalyst surface to produce the oxidation products, resulting in the reduction metal oxides. Secondaly, the reduced metal oxides are reoxidized by the gas phase oxygen. As schematically shown in Fig. 9, toluene is adsorbed on the active oxygen species on the catalyst surface, which occurs in the initiation by removing the α-H of methyl to form the benzoyl oxide species (C_6H_5—CH_2—O) (dark blue line), and then the reaction moves into subsequent oxidation steps (green line). Toluene is firstly converted to benzyl alcohol by lattice oxygen of the catalyst, then benzyl alcohol is further oxidized to benzoic acid, benzaldehyde and anhydride species on the surface of the catalyst, which are ultimately mineralized to CO_2 and H_2O to release into the atomsphere. In this case, the CuCZ/T catalyst seems to be a reservoir of oxygen species to sustain oxidation, and the Cu-Ce-O_{2-x} solid solution and CeO_2 can provide the significant oxygen vacancy. The lattice oxygen species are consumed for the oxidation of toluene and form oxygen vacancy, which can be replenished easily by the gas-phase oxygen activated on the catalyst surface (rose red line). This results can be explained by the coexistence of the mixed-valent Cu and the facile transform between Cu^{2+} and Cu^{+}, as shown from XPS results. And the presence of coupled Cu^{2+}/Cu^{+} sites with Ce^{4+}/Ce^{3+} sites can enhance the oxygen mobility throughout the bulk and the surface through electron exchange with cerium ions.

4. Conclusions

The catalytic self-sustained combustion of toluene over the CuCZ/T、CuMnCZ/T and MnCZ/T catalysts was investigated. The lean-combustion limits of toluene self-sustained combustion decrease with the improvement of the intrinsic catalyst activity. The results demonstrate that CuCZ/T is more efficient than others for toluene self-sustained combustion based on the lower T_{ig}, T_{co} and the lean-combustion limits. The performance enhancement of CuCZ/T is probably attributed to the homogeneous morphology, the high redox properties and the strong oxygen storage/release ability, because of the greater quantities of monovalent copper ions and lattice oxygen.

In-situ DRIFT results indicate the reaction pathway of the toluene catalytic oxidation. The active oxygen species are the adsorption sites

for the toluene oxidation. Toluene is adsorbed on the catalyst surface by abstracting a-H of the methyl group and forming benzoyl intermediates. These intermediates are oxidized successively into aldehydic, benzoate species, which are ultimately mineralized into CO_2 and H_2O. by the lattice oxygen in the catalyst.

Acknowledgments

This work was accomplished under the support of National Nature Science Foundation of China (No 51776216) and Research Centre of Modern Analytic Technology in Tianjin University of Science & Technology.

Appendix A. Supplementary data

Supplementary material related to this article can be found, in the online version, at doi:https://doi.org/10.1016/j.apcata.2018.10.034.

References

[1] S.C. Kim, W.G. Shim, Appl. Catal. B: Environ. 98 (2010) 180–185.
[2] W. Yang, Y. Wang, J. Zhou, Z. Wang, K. Cen, Chem. Eng. Sci. 158 (2017) 30–36.
[3] K. Bijjula, D.G. Vlachos, Proc. Combust. Inst. 33 (2011) 1801–1807.
[4] A. Scarpa, R. Pirone, G. Russo, D.G. Vlachos, Combust. Flame 156 (2009) 947–953.
[5] F. Bin, X. Wei, B. Li, K.S. Hui, Appl. Catal. B: Environ. 162 (2015) 282–288.
[6] F. Bin, X. Wei, T. Li, D. Liu, Q. Hao, B. Dou, Proc. Combust. Inst. 36 (2017) 4193–4200.
[7] Z. Huo, Transition Metal Oxides Nanostructures: Controlled Synthesis, Assembly and Their Properties, Tsinghua University, Beijing, 2009.
[8] N. Viswanadham, S.K. Saxena, A.H. Al-Muhtaseb, Mater. Today Chem. 3 (2017) 37–48.
[9] U. Menon, V.V. Galvita, G.B. Marin, J. Catal. 283 (2011) 1–9.
[10] H. Sun, Z. Liu, S. Chen, X. Quan, Chem. Eng. J. 270 (2015) 58–65.
[11] P. Liu, H. He, G. Wei, D. Liu, X. Liang, T. Chen, J. Zhu, R. Zhu, Microporous Mesoporous Mater. 239 (2017) 101–110.
[12] X. Li, L. Wang, Q. Xia, Z. Liu, Z. Li, Catal. Commun. 14 (2011) 11–19.
[13] X. Guo, J. Li, R. Zhou, Fuel 163 (2016) 56–64.
[14] H.C. Genuino, S. Dharmarathna, E.C. Njagi, M.C. Mei, S.L. Suib, J. Phys. Chem. C 116 (2012) 969–976.
[15] Q. Yang, Q. Hao, N. Yan, R. Zhao, C. Zhao, Q. Zhang, B. Dou, F. Bin, J. Fuel Chem. Tech. 45 (2017) 1401–1408.
[16] S. Li, Q. Hao, R. Zhao, D. Liu, H. Duan, B. Dou, Chem. Eng. J. 285 (2016) 536–543.
[17] B. Dou, S. Li, D. Liu, R. Zhao, J. Liu, Q. Hao, F. Bin, RSC Adv. 6 (2016) 53852-538553859.
[18] S. Hao, Y. Yin, Z. Ma, Y. Qing, F. He, Xi. Qi, J. Hebei Univ. (Nat. Sci. Ed. 25 (05) (2005) 486–494.
[19] Y. Wang, Research on Carbon Monoxide Self-sustained Combustion Based on $CuCe_{1-x}Zr_xO_y$ Series Catalyst, Xi'an: Xi'an Jiaotong University, 2016.
[20] X. Guo, J. Li, R. Zhou, Fuel 163 (2016) 056–064.
[21] L. Li, F. Jing, J. Yan, J. Jing, W. Chu, Catal. Today 297 (2017) 167–172.
[22] L. Liu, Basic Research of Catalytic Reduction of Nn by The Catalytic Reduction of Copper Oxide Nano-Catalyst in Cerium and Zirconia, Nanjing university, Nanjing, 2010.
[23] H. Lu, X. Kong, H. Huang, Y. Zhou, Y. Chen, J. Environ. Sci: China 32 (2015) 102–107.
[24] F. Hu, J. Chen, S. Zhao, K. Si, H. Song, J. Li, Appl. Catal. A Gen. 540 (2017) 57–67.
[25] V.P. Santos, M.F.R. Pereira, J.J.M. Órfão, J.L. Figueiredo, Appl. Catal. B: Environ. 99 (2010) 353–363.
[26] C. Deng, Q. Huang, X. Zhu, Q. Hu, W. Su, J. Qian, L. Dong, B. Li, M. Fan, C. Liang, Appl. Surf. Sci. 389 (2016) 1033–1049.
[27] R. Kang, X. Wei, F. Bin, Z. Wang, Q. Hao, B. Dou, Appl. Catal. A Gen. (2018), https://doi.org/10.1016/j.apcata.2018.07.026.
[28] B. Dou, G. Lv, C. Wang, Q. Hao, K. Hui, Chem. Eng. J. 270 (2015) 549–556.
[29] J. Li, H. Na, X. Zeng, T. Zhu, Z. Liu, Appl. Surf. Sci. 311 (2014) 690–696.
[30] Y. Liu, H. Huang, X. Li, S. Sun, D. Zhao, J. Saf. Environ. 5 (2005) 14–16.
[31] F. Rainone, D.A. Bulushev, L.K. Minsker, A. Renken, Phys. Chem. Chem. Phys. 5 (2003) 4445–4449.
[32] S. Besselmann, E. Löffler, M. Muhler, J. Mol. Catal. A Chem. 162 (2000) 401–411.